

To be published in the proceedings of the WEIN 1998 Conference

SEARCHES FOR NEW BOSONS COUPLING TO $e - q$ PAIRS AT HERA AND OTHER COLLIDERS

Y. SIROIS

*LPNHE Ecole Polytechnique, IN2P3-CNRS,
Palaiseau, France*

E-mail: sirois@polhp2.in2p3.fr

The early observation at HERA of an excess of events compared to the expectation from the Standard Model in very short distance e^+p deep-inelastic scattering processes has renewed the interest in the search for new physics which could manifest in electroweak-like interactions. New preliminary results from the H1 and ZEUS experiments making use of all available e^+p data are reviewed here, with an emphasis on the search for new bosons possessing Yukawa couplings to lepton-quark pairs. The sensitivity of HERA to leptoquarks, and to squarks of R-parity violating supersymmetry, is confronted to existing indirect constraints from rare and forbidden semi-leptonic decays, atomic parity violation and neutrinoless double-beta decay, as well as to direct constraints from LEP and Tevatron colliders. The HERA and Tevatron colliders are found to offer exciting prospects for new physics, accessing yet unexplored domains of the mass-coupling plane. Possible striking manifestation of explicit lepton flavour violation is also discussed.

1 Introduction

The interest in the search for a physics beyond the Standard Model (SM) which could interfere with electroweak-like interactions has been considerably enhanced recently by the observation in the H1¹ and ZEUS² experiments at HERA of a deviation from SM expectations in neutral current (NC) deep-inelastic scattering (DIS) events at very high squared momentum-transfer Q^2 and possibly, yet at a less significant level, in charged current (CC) processes. In particular, an apparent “clustering” of outstanding NC-like events at masses around 200 GeV has motivated considerable work on leptoquark constraints and phenomenology³ and on squarks in \tilde{R}_p -SUSY⁴, while contact interactions were also discussed as a possible source of distortion of the high Q^2 spectra⁵.

The ep collider HERA offers unique possibilities to search for s -channel production of new scalar particles which couple to lepton-parton pairs, up to a kinematic limit of $\sqrt{s_{ep}} \simeq 300$ GeV. The mass range relevant for a possible discovery at HERA has now been severely constrained by the TeVatron experiments^{6,7} in particular for scalars decaying with a large branching ratio β_{eq} into electron+quark. These constraints can be partly avoided for the squarks in \tilde{R}_p -SUSY theories where β_{eq} is naturally small given the competition with gauge decay modes. Exhaustive squark searches covering both \tilde{R}_p decay modes and various possible gauge decay modes are thus strongly motivated.

The original H1 and ZEUS results mentioned above were based on data samples collected from 1994 to 1996. The analyses have now been updated incorporating also the 1997 data, for a total gain of a factor $\simeq 2.5$ in integrated luminosity. New preliminary inclusive NC and CC HERA results using all available e^+p data will be reviewed in section 2 and 3 of this paper. Interpretation and constraints on contact interactions will be summarized in section 4. New results on leptoquark searches will be discussed in section 5 and searches for squarks of \tilde{R}_p -SUSY in section 6. Searches for direct lepton flavour violating processes will be discussed in the context of both leptoquark phenomenology and \tilde{R}_p -SUSY. The HERA results and prospects will be compared to those of indirect processes and to direct searches at other colliders.

2 New Physics and Very High Q^2 Rates at HERA

The investigations of very high Q^2 DIS-like processes at HERA, even with low statistics, are strongly motivated by the potential reach for new physics beyond the SM such as the production of new scalar (X_S) resonances. An X_S produced in the s -channel could for example lead to individual event signatures indistinguishable from standard NC and CC DIS if it decays into $e + q$ or $\nu + q$. The new signal would nevertheless be identified statistically as a peak in the invariant mass distribution, associated with a characteristic angular distribution of the decay products. As will be discussed in section 5, the X_S particles which decay uniformly in their CM frame would contribute most significantly at large Q^2 or large y where $Q^2 = M^2 y$, M is the resonance mass and y is related the decay polar angle of the final state lepton. Such new bosons possessing Yukawa couplings to lepton-quark pairs can in addition contribute in the u -channel by converting a lepton into a quark (and vice versa). Interference with SM DIS processes could also originate from effective contact interaction caused by the exchange of new bosons of masses $M \gg \sqrt{s_{ep}}$.

It is with these considerations in mind that H1 and ZEUS experiments have carried their original analysis^{1,2} of the 1994→96 data corresponding to integrated luminosities of $\mathcal{L}_{H1} \simeq 14.2 \pm 0.3 \text{ pb}^{-1}$ and $\mathcal{L}_{ZEUS} \simeq 20.1 \pm .5 \text{ pb}^{-1}$. The detailed comparison of the high Q^2 tail of NC and CC-like event rates with expectation from SM DIS processes has revealed exciting features. These observations have now been updated including 1997 data, for a total of $\mathcal{L}_{H1} \simeq 37 \text{ pb}^{-1}$ and $\mathcal{L}_{ZEUS} \simeq 46.6 \text{ pb}^{-1}$. I shall now briefly review the essential features of the original and updated rate measurements. The results obtained when “converting” the inclusive DIS measurements into differential cross-sections will be discussed in the next section.

The selection of NC-like events at HERA is straightforward. It essentially

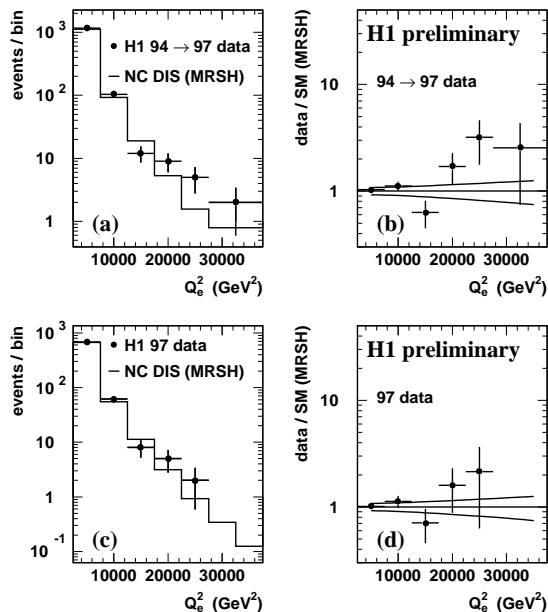


Figure 1: (a) Q_e^2 distribution of the NC DIS candidate events for the 1994→97 H1 data (●) and for standard NC DIS expectation (histogram); (b) ratio of the observed and expected number of events as a function of Q_e^2 ; the lines above and below unity specify the $\pm 1\sigma$ levels determined using the combination of statistical and systematic errors of the NC DIS expectation; (c) and (d) : as (a) and (b) but for 1997 data alone.

requires an isolated e^\pm at high $E_{T,e}$ well balanced by the hadronic transverse flow and with no longitudinal losses “visible” along the e beam $-z$ direction ($\sum_{vis.} E - P_z \simeq 2E_e^{beam}$). For any DIS-like event, as for the production of an X_S particle involved in a $2 \rightarrow 2$ body process, a mass $M = \sqrt{s_{ep}x}$ can be calculated. The Lorentz invariant x represents (at lowest order) the momentum fraction of the proton carried by the incident struck quark. By kinematic constraints, M and y (hence Q^2) can be reconstructed from two independent measurements such as the energy and angle of the final state lepton, or by combining two angles from the lepton and hadronic energy flow⁸.

Fig. 1a shows the Q_e^2 distribution measured⁹ by H1 for the 1994→97 data in comparison with the SM expectation for NC DIS. The ratio of the measured over expected distributions is shown in Fig. 1b. The essential features observed¹ in the original data remain visible. The NC DIS expectation is seen

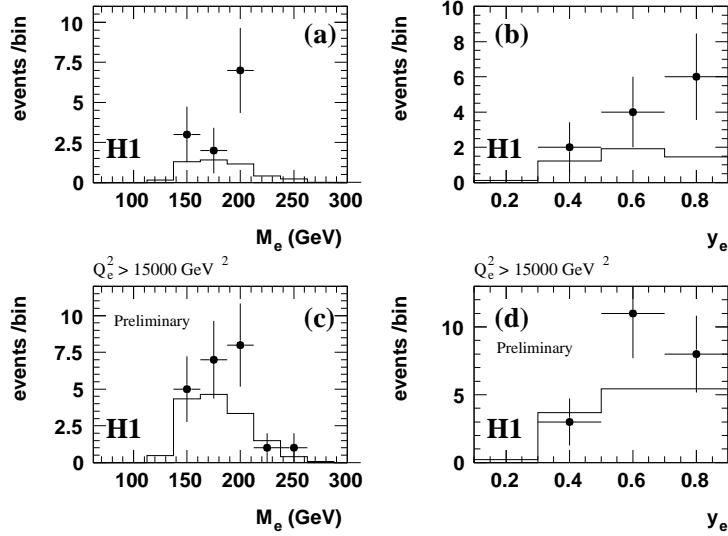


Figure 2: M_e and y_e distributions for H1 NC DIS candidate events (\bullet) at $Q_e^2 > 15000 \text{ GeV}^2$ for (a)(b) the 1994→96 data and (c) (d) the 1994→97 data. Superimposed as open histograms are the standard NC DIS expectation.

to be in excellent agreement with the data for $Q_e^2 \lesssim 10000 \text{ GeV}^2$. At larger Q_e^2 , deviations are observed, with a slight deficit in the range $Q^2 \simeq 10000 - 15000 \text{ GeV}^2$ and a number of observed events in excess at $Q^2 \gtrsim 15000 \text{ GeV}^2$. Similar plots are now shown in Fig. 1c,d for H1 1997 data alone. It is seen that the new data “suggests” similar deviations but with marginal significance. Considering the full set of e^+p data, H1 and ZEUS are left^{9,10} with slight excesses at highest Q^2 . For $Q^2 > 15000 \text{ GeV}^2$, H1+ZEUS observe $N_{obs}^{H1+ZEUS} = 42$ events while $N_{DIS} = 32 \pm 8.5$ events are expected. For $Q^2 > 20000 \text{ GeV}^2$, $N_{obs}^{H1+ZEUS} = 18$ while $N_{DIS} \simeq 9.5 \pm 1$. One expects an equal or larger upward fluctuation in $\sim 1\%$ of random experiments. ZEUS most significant Q^2 deviation comes from 2 outstanding events at $Q_{da}^2 > 35000 \text{ GeV}^2$ from their original dataset², where they now expect 0.29 ± 0.02 .

Fig. 2a and b show the H1 M_e and y_e distributions at $Q_e^2 > 15000 \text{ GeV}^2$ for the original 1994→96 dataset. The data was seen to exceed SM expectation most prominently around $M_e \sim 200 \text{ GeV}$ for large y_e . Out of the 12 H1 events at $Q^2 > 15000 \text{ GeV}^2$, 7 appeared to be “clustered” in the bin $200 \text{ GeV} \pm \Delta M/2$ with $\Delta M = 25 \text{ GeV}$ where one would expect 0.95 ± 0.2 . This particular clustering was not specifically supported by the original ZEUS observations¹¹.

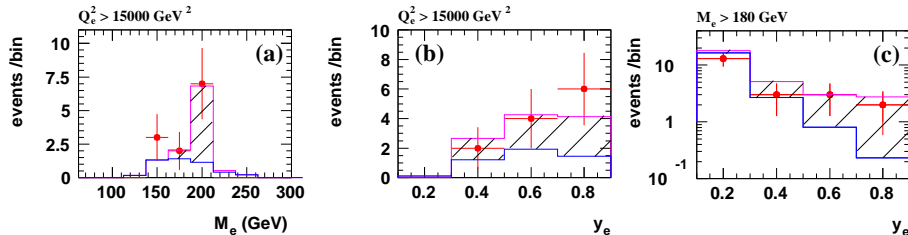


Figure 3: Same distributions as in Fig. 2 taken from ref. ¹ but showing in addition to NC DIS, as an illustration, the expectation for a $M = 200$ GeV scalar leptoquark.

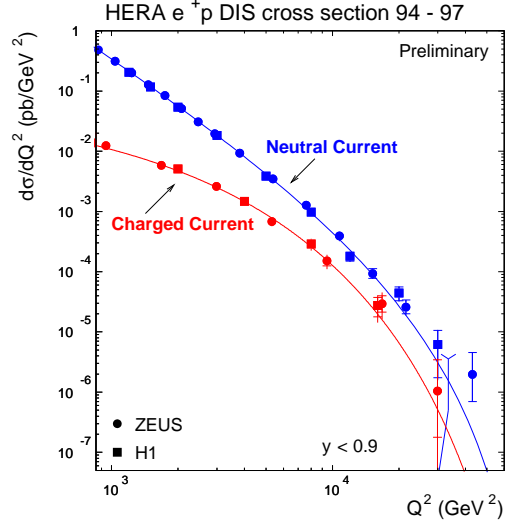
I will come back on this question in section 5. The same representation of H1 M_e and y_e results but including 1997 data are shown in Fig. 2c and d. The excess in the mass bin at $M \simeq 200$ GeV is found to be less significant. Here the full dataset was re-analysed including a new *in situ* electron energy calibration ^{12,13}. This has led to slight migrations (within originally quoted systematic errors) of individual events in the $M - y$ plane. In particular the M_e values are measured on average to be 2.4% higher. Considering nevertheless the same central mass bin of $200 \text{ GeV} \pm \Delta M/2$ with $\Delta M = 25$ where the most significant fluctuation was originally observed, H1 now finds $N_{obs} = 8$ events while $N_{DIS} = 3.0 \pm 0.5$ are expected. Of these observed events, 5 originate from the 1994 \rightarrow 96 data (for 38% of \mathcal{L}_{H1}) and 3 from the 1997 data (for 62% of \mathcal{L}_{H1}). Hence, it is fair to say that the “clustering” around $M_e \sim 200$ GeV is not confirmed by the 1997 data alone.

Shown for illustration in Fig. 3 are M_e and y_e contributions expected for a scalar leptoquark of mass $M_X = 200$ GeV and given coupling ¹³. Such a new particle would only contribute significantly at highest Q^2 . Hence, in presence or not of such new physics, it is reassuring that H1 and ZEUS have found ^{1,2} an excellent agreement between data and SM expectation for the y or mass spectra when considering low minimal Q^2 thresholds. Interestingly, at highest Q^2 the shape of the original M_e and y_e distributions and the excess are seen to be very well described by a combination of NC DIS + leptoquark contributions.

3 Differential Cross-Sections at High Q^2 at HERA

The observed Q_e^2 rates can be turned into differential cross-sections by converting the measured number of events to bin averaged values, using Monte Carlo acceptance calculations and detector efficiencies. It should be emphasized that such procedure implicitly assumes that the simulation of the SM model properly accounts for migrations (e.g. due to initial or final state gluon

Figure 4: Differential cross-section $d\sigma/dQ^2$ for NC and CC DIS processes measured by the H1 (squares) and ZEUS (points) with e^+p data and compared to SM expectation (using here CTEQ4 for the parton momentum distributions).

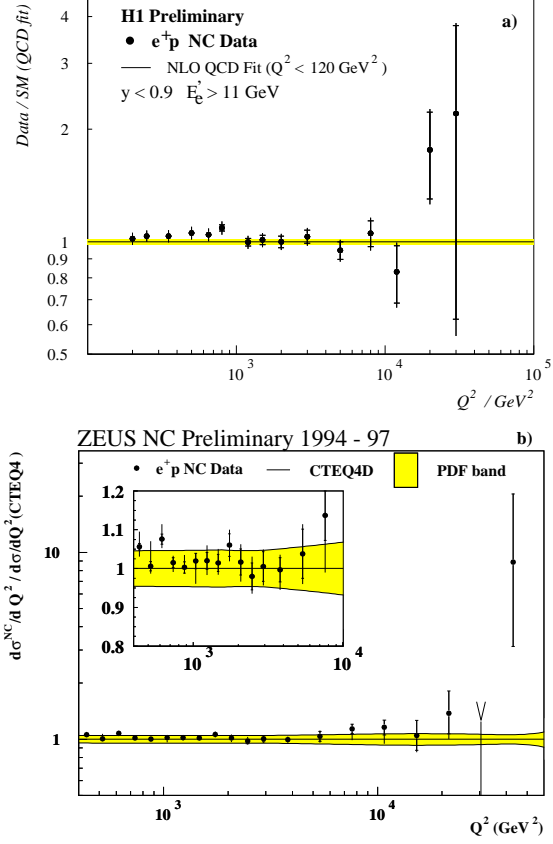


radiation) from true to measured kinematic quantities. This assumption could be invalidated in presence of new physics such as resonant production of long-lived leptomesons¹⁴. The differential cross-sections $d\sigma/dQ^2$ extracted by the H1⁹ and ZEUS experiments¹⁰ are shown for NC and CC DIS in Fig. 4.

Both experiments find for NC a remarkable agreement with SM expectation for $Q^2 \lesssim 10000 \text{ GeV}^2$ over 4 orders of magnitude. It should be recalled for completeness that in this Q^2 range and at large x , the SM contribution for NC DIS proceeds dominantly through t -channel γ -exchange with a u valence quark of the proton. For CC DIS, due to the W mass term in the exchanged boson propagator, the cross-section is suppressed at low Q^2 , and falls less steeply than for NC in the intermediate Q^2 range. In e^+p , CC proceeds dominantly through t -channel exchange with a d valence quark of the proton. Thus, the CC cross-section remains a factor $\gtrsim 4$ below that of NC for $Q^2 \gtrsim 10000 \text{ GeV}^2$.

Fig. 5a and b show for H1 and ZEUS the ratio of the measured over expected NC $d\sigma/dQ^2$ cross-sections. Here for the SM prediction, H1 performs⁹ a NLO QCD fit while ZEUS uses the CTEQ4 parton momentum distributions¹⁵. To constrain the high x domain, the H1 fit combines the F_2 structure function data from NMC¹⁶ and BCDMS¹⁷ on both proton and deuteron targets. It furthermore makes use of low Q^2 H1 data ($Q^2 \lesssim 120 \text{ GeV}^2$) from 1994 and 1995-96¹⁸. The measurement is clearly seen here to be in excellent agreement with SM expectation in the Q^2 range $1000 < Q^2 < 10000 \text{ GeV}^2$. As was already seen from “unbiased” event rates in Fig. 1, the H1 measurement slightly undershoots the SM expectation at $Q^2 \sim 10000 \text{ GeV}^2$ while an excess

Figure 5: Ratio of the measured over the SM predicted NC $d\sigma/dQ^2$ cross-section obtained by (a) H1 and (b) ZEUS. Here for the SM, H1 takes a NLO QCD fit extrapolated from $Q^2 \lesssim 120 \text{ GeV}^2$ data while ZEUS makes use of the CTEQ4D QCD evolved parton densities. The gray band shows (a) for H1 the uncertainty on the absolute normalisation (i.e. measured \mathcal{L}) and (b) for ZEUS the uncertainty on parton density functions. Inner (outer) bars correspond to statistical (total) errors.



is observed at the 2σ level for $Q^2 \gtrsim 15000 \text{ GeV}^2$. For CC DIS, H1 and ZEUS had observed in their original analysis^{1,2} and still observe^{10,12,19} a tendency for the data to lie above SM expectation at highest Q^2 ; but the CC results receive large systematic error contributions from the experiments (hadronic energy scale) and “model” (d quark momentum density). For a measured $Q_h^2 > 15000 \text{ GeV}^2$, H1 observes 9 events for 5.1 ± 2.8 expected while ZEUS observes 8 events for $3.9^{+1.9}_{-1.6}$ expected.

The $d^2\sigma/dxdQ^2$ cross-section extracted by H1 is plotted as a function of Q^2 for a wide range of fix x values in Fig. 6. The results are expressed in terms of the reduced cross-section $\tilde{\sigma}_{NC}$ defined as $\tilde{\sigma}_{NC} \equiv (xQ^4/2\pi\alpha^2) 1/(1 + (1 - y)^2) d^2\sigma/dxdQ^2$. They are compared to the MRST structure function fit extrapolated to high Q^2 as well as to a NLO QCD fit⁹ taking into account the H1 high Q^2 data. The high Q^2 data is seen to further pull the NLO QCD fit

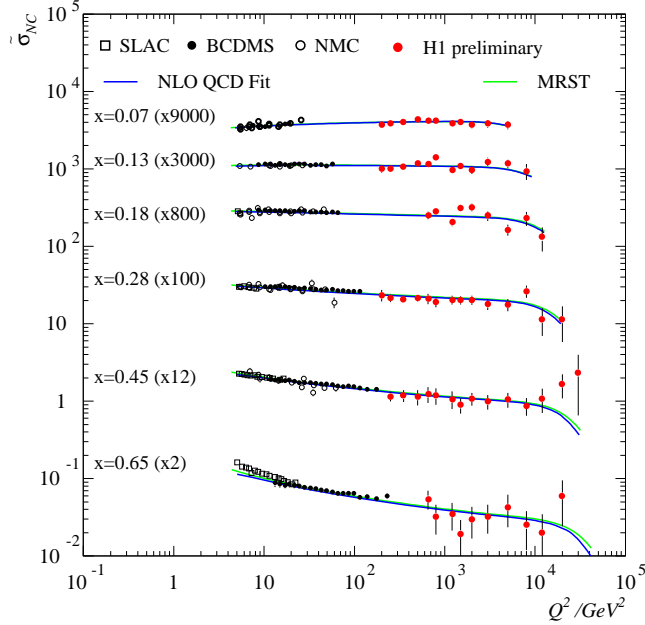


Figure 6: Measured H1 $d^2\sigma/dxdQ^2$ reduced NC cross-section (\bullet) compared to the MRST parametrization (upper curves) and to a new NLO QCD fit (lower curves) combining H1 preliminary results with BCDMS and NMC.

downward at highest Q^2 relative to MRST. The upward “fluctuation” discussed above is, here consistently, visible at $x \simeq 0.45$ and $Q^2 \gtrsim 15000 \text{ GeV}^2$. From an analysis²⁰ of the $d\sigma/dx$ cross-section for $Q^2 > 10000 \text{ GeV}^2$, and for the bulk of the cross-section which sits at the intermediate x range of $x \simeq 0.2 - 0.3$, the suppression due to the negative $\gamma - Z^0$ interference in e^+p collisions (strikingly manifest from the inflexion of the theoretical prediction in Fig. 6) has now been solidly confirmed by both HERA experiments^{10,12}.

4 Searches for Contact Interactions

Through the interference with SM gauge boson exchange, new bosons of mass $M \gg \sqrt{s_{ep}}$ could affect the $d\sigma/dQ^2$ cross-section measurements at HERA. Such a new interaction can be described as an effective 4-fermion “pointlike” $(\bar{e}e)(\bar{q}q)$ contact interaction (CI). CI was discussed⁵ as a possible “explanation” of an excess of very high Q^2 events at HERA. The sensitivity to CI has now

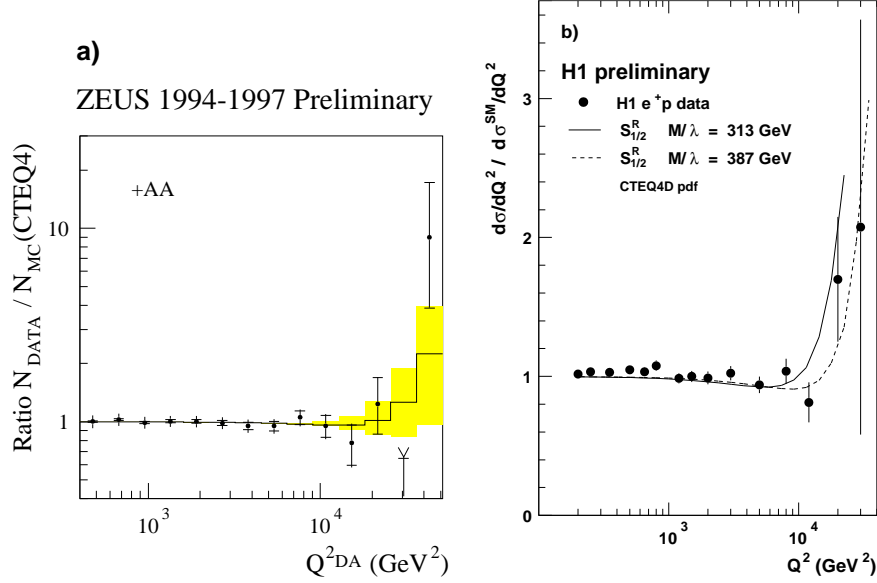


Figure 7: (a) Ratio of the number of observed events per Q^2 interval in ZEUS to the SM expectation. The full line shows the contact interaction (CI) best fit for the +AA model (see text); the shaded area is bounded by the $\pm 1\sigma$ limits. (b) Ratio of the measured $d\sigma/dQ^2$ to the SM expectation for NC-like events in H1; the full line (dashed line) gives for a CI the 95% CL (resp. the CI best fit) for the $S_{1/2}^R$.

been investigated²² using all available e^+p data and considering the interaction Lagrangian $\mathcal{L}_{int} = \mathcal{L}_{SM}^{NC} + \mathcal{L}_{CI}^{NC}$ where the chiral invariant \mathcal{L}_{CI}^{NC} complementing the SM can be written in the form $\mathcal{L}_{CI}^{NC} = \sum \{ \eta_{ij}^q (\bar{e}_i \gamma_\mu e_i) (\bar{q}_j \gamma^\mu q_j) \}$ with $q = u, d$ and $i, j = L, R$ and the coupling coefficients defined as $\eta_{ij} \equiv \pm g^2 / \Lambda_{ij}^{\pm 2}$. The + (−) sign indicate constructive (destructive) interference. The “mass scale” Λ^\pm is conventionally defined when setting constraints as that scale relevant for a “strong” coupling strength of $g^2 = 4\pi$.

The chirality structure of the CI model can be chosen to avoid the severe constraints coming from atomic parity violation²¹ (APV). These are cancelled in particular if for the quarks q , $\eta_{LL}^q + \eta_{LR}^q - \eta_{RL}^q + \eta_{RR}^q = 0$, as realized for instance in the VV , AA and VA models considered by H1 and ZEUS, with the mixture $VV = LL + LR + RL + RR$, $VA = LL - LR + RL - RR$, and $AA = LL - LR - RL + RR$. The SU(2) invariance is assumed which imposes $\eta_{LL}^u = \eta_{LL}^d$ and $\eta_{RL}^u = \eta_{RL}^d$.

Table 1: Constraints at 95% CL on contact interaction scale Λ from HERA and other colliders in models with VV, AA or VA structure (see text) for constructive (Λ^+) or destructive (Λ^-) interference.

Model		95% CL Lower Limits			
		HERA		TeV	LEP
		H1	ZEUS	CDF/D0	ADLO
VV	Λ^+	4.5	4.9	3.5	4.0
	Λ^-	2.5	4.6	5.2	5.2
AA	Λ^+	2.0	2.0	3.8	5.6
	Λ^-	3.8	4.0	4.8	3.7
VA	Λ^+	2.6	2.8		
	Λ^-	2.8	2.8		

Figure 7a shows CI constraints and best fit to the Q^2 spectrum obtained by ZEUS for the $AA(\Lambda^+)$ scenario. Figure 7b shows as an illustration the constraints and best fit obtained by H1 in a leptoquark $S_{1/2}^R$ scenario. The $S_{1/2}^R$ (see nomenclature in next section) possesses a $-5/3$ charge state coupling to $e_R^- \bar{u}$ ($e_L^+ u$) and a $-2/3$ charge state coupling to $e_R^- \bar{d}$ ($e_L^+ d$). Assuming SU(2) invariance, the CI couplings are $\eta_{RL}^u = \eta_{RL}^d = -1/2(\lambda/M_S)^2$. Both experiment rightly conclude²² independently that no significant indication of a CI was found for these and various other models considered²². It is nevertheless interesting to note that the best fits in the $AA(\Lambda^+)$ scenario are found, consistently, to allow for a non-vanishing coupling. ZEUS finds $\eta/4\pi = 1/\Lambda_0^2 = 0.16_{-0.06}^{+0.05}$ while H1 finds $0.15_{-0.07}^{+0.04}$; corresponding roughly to a value of $\Lambda_0 \simeq 2.5$ TeV. In practice, such a simple CI scenario is actually ruled out by TeVatron and LEP constraints as seen in Table 1. It is also interesting to note that, as seen in Fig. 7b an hypothetical scalar can be accommodated by H1 data for $M_S/\lambda = 387$ GeV. For the VV and VA scenario, the HERA sensitivity is found to be comparable to that of other colliders. The $VV(\Lambda^-)$ scenario would lead to a suppression of the NC $d\sigma/dQ^2$ up to a few 10^4 GeV² followed by a strong enhancement²² qualitatively similar to the actual observation.

5 Searches for Leptoquarks and Lepton Flavour Violation

Generic leptoquarks (LQ) are colour triplet bosons which appear naturally in various unifying theories beyond the SM such as Grand Unified Theories and Superstring inspired E_6 models, and in some Compositeness and Technicolour models. LQ searches have been carried either in the strict context of the original Buchmüller-Rückl-Wyler (BRW) effective model²³ where the decay

$F = -2$	Prod./decay	$\mathcal{B}(e^+q)$	$F = 0$	Prod./decay	$\mathcal{B}(e^+q)$
$^{-1/3}S_0^*$	$e_R^+\bar{u}_R \rightarrow e^+\bar{u}$	1/2	$^{-5/3}S_{1/2}^*$	$e_R^+u_R \rightarrow e^+u$	1
	$e_L^+\bar{u}_L \rightarrow e^+\bar{u}$	1		$e_L^+u_L \rightarrow e^+u$	1
$^{-4/3}\tilde{S}_0^*$	$e_L^+\bar{d}_L \rightarrow e^+\bar{d}$	1	$^{-2/3}S_{1/2}^*$	$e_L^+d_L \rightarrow e^+d$	1
$^{-4/3}S_1^*$	$e_R^+\bar{d}_R \rightarrow e^+\bar{d}$	1	$^{-2/3}\tilde{S}_{1/2}^*$	$e_R^+d_R \rightarrow e^+d$	1
$^{-1/3}S_1^*$	$e_R^+\bar{u}_R \rightarrow e^+\bar{u}$	1/2			

Table 2: Scalar leptoquarks isospin families in the Buchmüller-Rückl-Wyler model. These LQ will be in the following indexed with the chirality of the incoming *electron* which could allow their production, e.g. the \tilde{S}_0^* will be denoted by $\tilde{S}_{0,R}^*$.

branching ratios are fixed by the model, or in the context of generic models allowing for arbitrary branching ratios.

The BRW model considers all possible scalar (S_I) and vector (V_I) LQs of weak isospin I with dimensionless Yukawa couplings $\lambda_{ij}^{L,R}$ to lepton-quark pairs, where i and j indices denote lepton and quark generations respectively and L or R is the chirality of the lepton. The general effective Lagrangian obeys the symmetries of the SM and introduces 10 different LQ isospin multiplets, among which 5 are scalar families. These are listed in Table 2 in the so-called Aachen nomenclature and classification scheme²⁴. The LQ search can be restricted to pure chiral couplings of the LQs given that deviations from lepton universality in helicity suppressed pseudoscalar meson decays have not been observed²⁵. This restriction to couplings with either left- (λ^L) or right-handed (λ^R) leptons (i.e. $\lambda^L \cdot \lambda^R \sim 0$), affects only two scalar LQs (S_0 and $S_{1/2}$). In all the results presented below, it is implicitly assumed as a simplifying assumptions that one of the LQ isospin doublet or triplet is produced dominantly and that the mass eigenstates within this multiplet are degenerate.

5.1 Search for first generation leptoquarks

The search for first generation LQs at HERA involves the analysis of DIS-like events at very high Q^2 . The production cross-section σ_{LQ} depends on the quark momentum density in the proton and approximately scales with λ^2 . The scalar resonance which can then decay into $e + q$ or $\nu + q$ is expected to have a very narrow intrinsic width $\Gamma = \lambda^2 M / 16\pi$ and the decays into a lepton and a quark jet lead to event signatures indistinguishable from SM DIS. A characteristic statistical signal of the direct production of LQs in the s -channel would be a peak in the reconstructed mass distribution. The LQ mass can be

reconstructed from the decay products (e.g. a charged lepton and a jet) or from kinematic constraints as $M = \sqrt{s_{ep}x}$. The isotropic decay of the LQs in their CM frame leads to a flat y spectrum. In this frame $y = \frac{1}{2}(1 + \cos\theta^*)$ with θ^* being the decay polar angle of the final state lepton. This is markedly different from the $d\sigma/dy \sim y^{-2}$ distribution expected at fixed x for the dominant t -channel γ -exchange in NC DIS events. Hence, the signal of first generation LQs would be most prominent at high y or equivalently at large $Q^2 = M^2y$.

The H1 LQ search for NC-like events requires an isolated e^+ with a transverse energy of $E_{T,e} > 15$ GeV. The reconstruction of the kinematics relies essentially (except for about $\simeq 4.4\%$ of azimuthal range) on the e^+ energy and angle. The mass and y values of all events with $Q^2 > 2500$ GeV² are shown in Fig. 8(*top left*). The corresponding measured mass spectrum shape is found to be very well predicted by the SM as can be seen in Fig. 8(*top right*). Also shown there are the mass spectra after having applied a mass dependent y cut⁹ designed via Monte Carlo studies to optimize the signal significance for scalar LQ searches. This cut varies from $\simeq 0.6$ at $M_e \simeq 60$ GeV to $\simeq 0.4$ at $M_e \simeq 200$ GeV, and down to $y_e \simeq 0.2$ at $M_e \gtrsim 250$ GeV. H1 observes 312 events satisfying this y cut in the mass range $M_e > 62.5$ GeV, in excellent agreement with the SM expectation of 306 ± 23 . In the mass range $200 \text{ GeV} \pm \Delta M/2$ with $\Delta M = 25$ GeV, $N_{obs} = 8$ events are found for $N_{DIS} = 3.0 \pm 0.5$. As was discussed in section 2, this slight excess mostly originates from the 1994→96 dataset. These 8 events have an average mass of $M_e \simeq 206$ GeV. When discussing sensitivity and constraints on LQ searches, it should be kept in mind that according to LQ Monte Carlo simulations, the mass M_e as deduced from the positron tends to systematically underestimate a true LQ mass by $\sim 2\%$ for M_{LQ} of $\mathcal{O}(200 \text{ GeV})$. The most significant fluctuation is observed in H1 for M_e values which would correspond to $M_{LQ} \simeq 210$ GeV.

The ZEUS LQ search for NC-like events requires a total $E_T \geq 60$ GeV. A mass M_{eJ} is attributed to each candidate event and calculated from the positron and the jet at highest E_T , not correcting for the finite jet mass. The M_{eJ} and $\cos\theta^*$ for all events are given in Fig. 8(*bottom left*). Interestingly, the outstanding high Q^2 events already discussed in ref.² here tend to cluster around $M_{eJ} \simeq 215$ GeV. The projected M_{eJ} spectrum is shown in Fig. 8(*bottom right*) after having applied conservatively a fiducial cut (shaded area in Fig. 8(*bottom left*)) which removes a difficult region for electron energy measurements at the interface between two calorimeters, thus cutting away 2 very high Q^2 events. In the remaining acceptance and for $M_{eJ} > 200$ GeV and $\cos\theta^* > 0.25$, ZEUS observes 7 events in slight excess of the SM expectation of 4.3 events. Of these 7 events, 5 originate from the 1994→96 dataset. For $M_{eJ} > 200$ GeV and in the full $\cos\theta^*$ range, 68 events are observed for an ex-

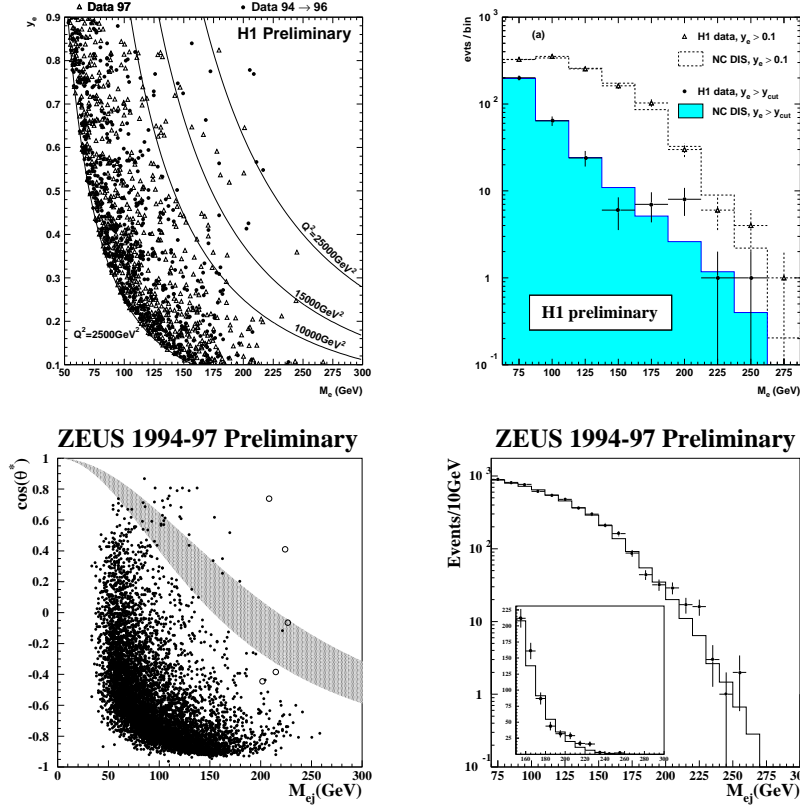
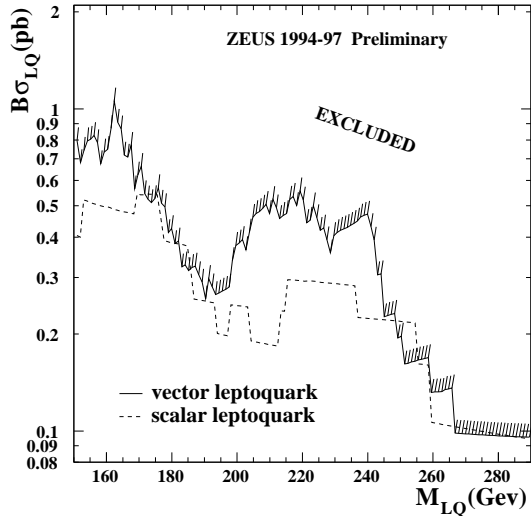


Figure 8: NC DIS candidate events in the y - M plane (left) and mass spectra (right) from H1 (top) and ZEUS (bottom).

pectation of 43^{+14}_{-12} from SM. This excess is found by ZEUS¹⁰ to be mostly due to events having a $\cos \theta^*$ spectrum shape compatible with SM DIS expectation.

While interesting upward fluctuations of the number of observed events have been found by both H1 and ZEUS for masses $M \gtrsim 200$ GeV in their 1994→96 dataset, the 1997 data disappointingly offered no confirmation of an excess in the NC DIS-like channel which would possess the characteristics of lepton-quark resonant production. Hence, both experiments proceed to set mass dependent constraints on the production cross-section σ_{LQ} of first generation scalar LQs, treating the deviations observed as statistical fluctuations. Model “independent” upper limits on σ_{LQ} were derived by ZEUS in ref.¹⁰ and are shown in Fig. 9.

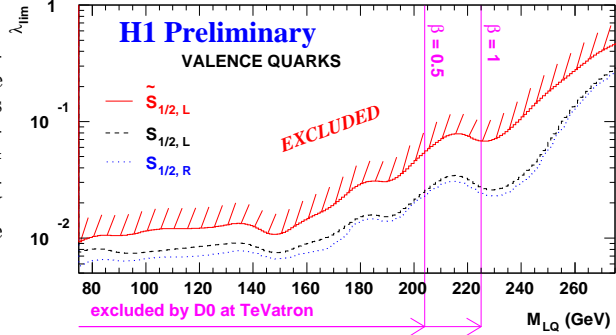
Figure 9: Cross-section exclusion limits at 95% CL from ZEUS for generic scalar and vector leptoquarks.



Further interpretation of such constraints can be discussed in the framework of the BRW model²³ where β_{eq} values are fixed by the model for the various LQ types, as given e.g. for scalars in Table 2. The exclusion upper limits on σ_{LQ} translated into mass dependent limits on λ_{11} as obtained by H1 are shown in Fig. 10 for scalar LQs having fermionic number $F = 0$, i.e. which can be produced via a fusion between the e^+ and a u or d valence quark. The limits are given here for masses up to 275 GeV above which one needs to move away from a resonance-like search since the mass peak of $F = 0$ scalars becomes severely distorted. Very similar results are obtained by ZEUS who also derived constraints for vector LQs¹⁰. The e^+p collisions naturally offers the best sensitivity to $F = 0$ LQs and the limits obtained represent an improvement by a factor $\simeq 3$ compared to previously published HERA results²⁶. For a coupling of the electromagnetic strength $\lambda^2/4\pi = \alpha_{EM}$ (i.e. $\lambda \simeq 0.3$), such LQ are excluded at 95% CL up to 275 GeV. The highest sensitivity (hence most severe constraints) is obtained for $S_{1/2}^R$ since both charge states can be produced via a e^+u and e^+d fusion. Only e^+u (e^+d) fusion is possible for the s -channel production of $S_{1/2}^L$ ($\tilde{S}_{1/2}^L$). The $F = 2$ LQs will be best probed with the forthcoming e^-p data taking starting in 1998 at HERA.

The mass range of interest for a possible discovery at HERA of a LQ of the strict BRW model has now been severely reduced by the TeVatron $p\bar{p}$ experiments^{6,7}, where first generation scalar LQs with $M < 242$ GeV and $\beta_{eq} = 1$ are excluded (95% CL) independently of the λ (see ref. ²⁷). For

Figure 10: Exclusion limits at 95% CL on the Yukawa coupling λ as a function of the leptoquark mass for $F = 0$ scalar leptoquarks described by the BRW model. Domains above the curves are excluded.



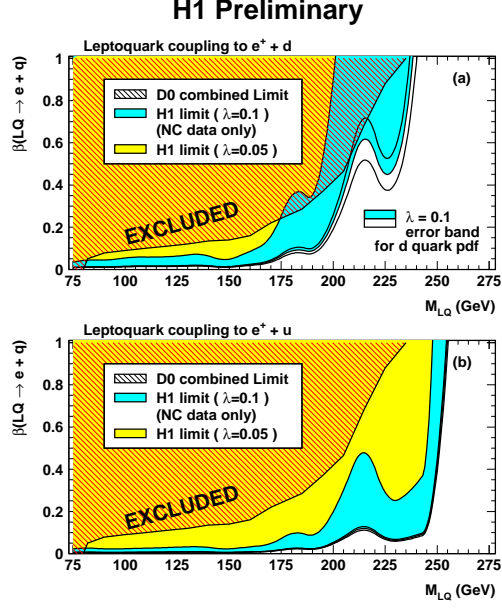
$\beta_{eq} = 0.5$, the excluded domain reaches $M \simeq 200$ GeV. The mass range excluded by the D0 experiment alone is shown in Fig. 10. At LEP e^+e^- collider, searches²⁸ for single LQs using data taken at centre of mass energies of 161 and 172 GeV gives for $\lambda \simeq 0.3$ a best resulting limit of 142 GeV which is not yet competitive with the sensitivity achieved at HERA.

Moving away from the BRW model, one can consider from a phenomenological point of view scalar LQs undergoing both NC and CC DIS-like decays ($\beta_{eq} \times \beta_{\nu q'} \neq 0$) with β_{eq} and $\beta_{\nu q'}$ treated as free parameters. By gauge invariance this can only be relevant for LQ coupling to $e^+\bar{u}$. H1 has derived⁹ such constraints. For $\beta_{\nu q'} = 90\%$ and $\beta_{eq} = 10\%$, LQ masses below 210 GeV are found to be excluded at 95% CL for a coupling $\lambda_{11} \simeq 0.3$. This extends far beyond the domain excluded by TeVatron experiments^{6,7} which for such small values of β_{eq} only exclude scalar LQ masses below $\simeq 110$ GeV. Given a value of λ_{11} , upper limits on σ_{LQ} can be translated for narrow intrinsic widths in terms of mass dependent limits on the branching β_{eq} without making specific assumptions on the nature of the other decay modes. Results are shown in Fig. 11a and b for LQs produced via e^+d and e^+u fusion respectively. Despite the small λ_{11} values considered, the exclusion domains are seen in Fig. 11 to extend beyond the region covered by the $D\bar{0}$ experiment⁶ at TeVatron for small β_{eq} even in the less favourable case of an LQ coupling to e^+d . HERA rules out masses below $\simeq 210$ GeV if $\lambda_{11} = 0.1$ (Fig. 11b) or below $\simeq 255$ GeV for a interaction of electromagnetic strength (see for instance Fig. 12a).

5.2 Search for leptoquarks with mixed lepton flavour couplings

We have seen in the previous section that the mass range of interest for a discovery of lepton-quark resonances at HERA is severely constrained by TeVatron results for LQs coupling solely to first generation fermions. Hence, H1

Figure 11: Mass dependent exclusion limits at 95% CL on the branching ratio $\beta_{eq} = BR(LQ \rightarrow eq)$ for scalar leptoquarks produced by (a) e^+d and (b) e^+u fusion. Two exclusion regions (light dotted grey) corresponding to $\lambda = 0.1$ and $\lambda = 0.05$ are represented. The $D\emptyset$ limit is also shown as hatched region.



has investigated⁹ further the case of LQs possessing $\lambda_{11} \times \lambda_{3j} \neq 0$. Such a LQ coupling to both first and third generation leptons would lead to striking lepton flavour violating (LFV) processes $e^+q \rightarrow LQ \rightarrow \tau^+q'$.

The analysis for the $LQ \rightarrow \tau + q$ decays covers the hadronic decays of the τ as well as the decay $\tau^+ \rightarrow \mu^+\nu_\mu\bar{\nu}_\tau$ but only the former is actually used in the exclusion limits derivation. For the latter, the analysis requires simply an isolated track with transverse momentum $P_T > 10$ GeV linked to the primary vertex and a visible transverse momentum flow imbalance as measured solely via calorimetry of $P_{T,miss}^{vis.} > 25$ GeV. Only four μ +jet events are found to satisfy these criteria. All four are amongst the “outstanding” high P_T lepton events discussed in ref.²⁹. None of these $\mu + X$ events has a μ candidate at θ_μ and ϕ_μ angles corresponding to the τ angles predicted from kinematical constraints (the μ from the τ decay should be strongly boosted in the τ direction). Hence neither $LQ \rightarrow \mu + q$ (2^{nd} generation) nor $LQ \rightarrow \tau + q$; $\tau \rightarrow \mu\nu\bar{\nu}$ (3^{rd} generation, μ channel) candidates are found. For the hadronic decays of the τ , the analysis requires a “pencil-like” jet defined by a small invariant mass $M_{jet} \leq 7$ GeV and a low multiplicity of associated charged tracks ($N_{tracks} \leq 2$). The τ jet furthermore must have either a large intrinsic π^0 component or a stiff leading track, and be back-to-back in azimuth with the

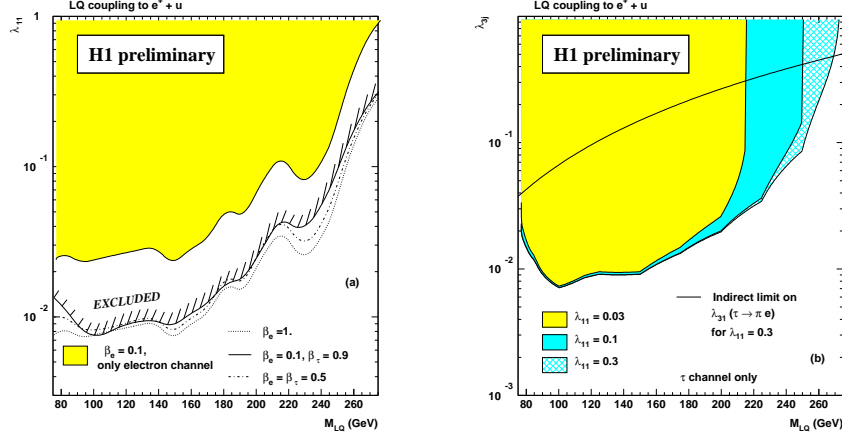


Figure 12: (a) M_{LQ} dependent exclusion limits at 95% CL on the Yukawa coupling λ_{11} , for scalar leptoquarks produced by e^+u fusion. Different hypothesis for the branching ratios into $eq, \tau q$ are considered. Domains above the curves are excluded. (b) Exclusion domains in the plane λ_{3j} ($j = 1, 2$) against M_{LQ} for several fixed value of λ_{11} (greyed areas). Indirect limits on λ_{31} are represented by the dotted curve.

rest of the hadronic flow. No candidate is found for these τ hadronic decay modes while 0.8 ± 0.3 misidentified background event is expected.

Mass dependent exclusion limits are shown for λ_{11} in Fig. 12a when fixing the relative β_{eq} and $\beta_{\tau q}$ branching fractions for a generic LQ coupling to $e^+ + u$ pairs (such as the $S_{1/2,L}^*$ in the BRW model) and for three different sets of $(\beta_{eq}, \beta_{\tau q})$. Here both channels $LQ \rightarrow e^+ + jet$ and $LQ \rightarrow \tau^+ + jet$ are combined. This latter channel is essentially background free but the former benefits from a higher selection efficiency, such that both provide comparable sensitivity. Hence, when $\beta_{eq} + \beta_{\tau q} \simeq 1$, the exclusion domain is very similar to the one obtained for $\beta_{eq} = 1$. Assuming $\beta_{eq} = 10\%$ and $\beta_{\tau q} = 90\%$, masses below 275 GeV are excluded at 95% CL for $\lambda_{11} = \sqrt{4\pi\alpha}$ as shown in Fig. 12a. An alternative representation of the LFV constraints is given in Fig. 12b in the plane λ_{3j} against M_{LQ} for different fixed values of λ_{11} . Here again, a LQ formed via e^+u fusion is considered such that only couplings λ_{3j} with $j = 1, 2$ are relevant. Furthermore the simplifying assumption $\beta_{eq} + \beta_{\tau q} = 1$ is made. Fig. 12b shows the domains excluded at 95% CL by the $\tau + jet$ final states analysis. Of course, for each hypothetical value of λ_{11} , part of the mass and $\lambda_{11} \times \lambda_{3j}$ domain is already implicitly excluded anyway by

the $e + q$ analysis alone. Nevertheless, the $\tau + jet$ analysis allows extend considerably the coverage of possible $\lambda_{11} \times \lambda_{3j}$ values; e.g. for $\lambda_{11} = 0.03$ (1/100 of electromagnetic strength) the mass range above $M_{LQ} \simeq 80$ GeV is covered in complement. For $\lambda_{11} = \lambda_{3j} = 0.03$, these new HERA results extends the mass limits from previous HERA results³² by $\simeq 65$ GeV.

The best indirect constraint²⁵ on λ_{31} , shown in Fig. 12b in the case $\lambda_{11} = 0.3$, is found to be typically one order of magnitude less stringent than HERA exclusion limit. This constraint comes from the upper limit on the branching ratio $\beta_{\tau \rightarrow \pi^0 e}$ which could be affected by the process $\tau \rightarrow d + LQ^*$; $LQ^* \rightarrow e + d$. No low energy process constrains the coupling λ_{32} . Thus, a domain which was yet unexplored is now covered by H1 in the plane λ_{32} against M_{LQ} . It should be noted however that other LQ species might suffer more severely from indirect constraints. This is the case in particular of LQs coupling to e^+d pairs (such as the $\tilde{S}_{1/2,L}$ in BRW model) for which the the couplings λ_{31} , λ_{32} or λ_{33} are constrained respectively by $\tau \rightarrow \pi^0 e$, $\tau \rightarrow K^0 e$ and $B \rightarrow \tau e X$ ²⁵. Such LQs have characteristics similar to the \tilde{u}_L^j squark in SUSY models where R-parity is violated (see next section) by couplings λ'_{1j1} (analogous to λ_{11}) and λ'_{3jk} (analogous to λ_{3k}). Exclusion domains which have been derived in³³ in the plane λ'_{3jk} against $M_{\tilde{u}}$ show that even in such a case, HERA sensitivity extends beyond that of low energy phenomena for masses $M_S \lesssim 250$ GeV.

The CDF experiment has performed a search for third generation LQ looking at $\tau\tau b\bar{b}$ final states³⁰, and excludes a scalar LQ with masses below 99 GeV if $\beta_{\tau b} = 1$. A complementary search has been carried out by $D\bar{0}$ ³¹, where the analysis of $\nu\nu b\bar{b}$ final states leads to a lower mass limit of 94 GeV for $\beta_{\nu b} = 1$. These constraints are less stringent than the $\simeq 110$ GeV mass limit obtained from TeVatron searches for first generation LQs assuming $\beta_{eq} = 10\%$. Thus, a situation with small β_{eq} and large $\beta_{\tau q}$ is especially favourable, leaving open e.g. for HERA an important discovery window at $M_{LQ} \lesssim \sqrt{s_{ep}}$.

6 Searches for Squarks of R -parity Violating Supersymmetry

Squarks are scalar SUSY partners of the quarks. The most general SUSY theory which preserves gauge invariance of the Standard Model (SM) allows for Yukawa couplings between one scalar squark (\tilde{q}) or slepton (\tilde{l}) and two known SM fermions. Such couplings induce violation of the R -parity defined as $R_p = (-1)^{3B+L+2S}$, where S denotes the spin, B the baryon number and L the lepton number of the particles. Of special interest for HERA³⁴ are those Yukawa couplings λ'_{1jk} (j, k are generation indices) violating the leptonic number and which couple to a squark to a lepton-quark pair. The search for R_p -SUSY at HERA was carried³³ considering otherwise the field content of

Table 3: Squark production processes at HERA (e^+ beam) via a R -parity violating λ'_{1jk} coupling.

λ'_{1jk}	production process	
111	$e^+ + \bar{u} \rightarrow \tilde{d}_R^*$	$e^+ + d \rightarrow \tilde{u}_L$
112	$e^+ + \bar{u} \rightarrow \tilde{s}_R^*$	$e^+ + s \rightarrow \tilde{u}_L$
113	$e^+ + \bar{u} \rightarrow \tilde{b}_R^*$	$e^+ + b \rightarrow \tilde{u}_L$
121	$e^+ + \bar{c} \rightarrow \tilde{d}_R^*$	$e^+ + d \rightarrow \tilde{c}_L$
122	$e^+ + \bar{c} \rightarrow \tilde{s}_R^*$	$e^+ + s \rightarrow \tilde{c}_L$
123	$e^+ + \bar{c} \rightarrow \tilde{b}_R^*$	$e^+ + b \rightarrow \tilde{c}_L$
131	$e^+ + \bar{t} \rightarrow \tilde{d}_R^*$	$e^+ + d \rightarrow \tilde{t}_L$
132	$e^+ + \bar{t} \rightarrow \tilde{s}_R^*$	$e^+ + s \rightarrow \tilde{t}_L$
133	$e^+ + \bar{t} \rightarrow \tilde{b}_R^*$	$e^+ + b \rightarrow \tilde{t}_L$

the Minimal Supersymmetric Standard Model (MSSM) and assuming that the neutralino χ_i^0 is the lightest supersymmetric particle (LSP).

Production and decay: With an e^+ in the initial state, each of the nine λ'_{1jk} coupling allows for a resonant production of squarks through a $e - q$ fusion process listed in Table 3. The squarks decay either via their λ' coupling into SM fermions, or via their gauge couplings into a quark and a neutralino χ_i^0 ($i = 1, 4$) or a chargino χ_j^\pm ($j = 1, 2$). The mass eigenstates χ_i^0 and χ_j^\pm are mixed states of gauginos and higgsinos and are in general unstable. This latter point holds in \tilde{R}_p -SUSY, in contrast to the strict MSSM, also for the LSP which decays via λ'_{1jk} into a quark, an antiquark and a lepton. In cases where both production and decay occur through a λ'_{1jk} coupling (e.g. Fig. 13a and c for $\lambda'_{111} \neq 0$), the squarks behave as scalar LQs. The \tilde{d}_R^{k*} can decay either into $e^+ + \bar{u}^j$ or $\nu_e + \bar{d}^j$. Gauge invariance forbids the $\tilde{u}_L^j \rightarrow \nu q$ decay and, hence, such squark type is left in the \tilde{R}_p decay mode with $\tilde{u}_L^j \rightarrow e^+ + d^k$. Hence, the final state signatures consist of a lepton and a jet and are, event-by-event, indistinguishable from the SM neutral and charged current DIS. In cases where the \tilde{u}_L^j (resp. \tilde{d}_R^{k*}) undergoes a gauge decay into a χ_α^0 or a χ_β^\pm (resp. χ_α^0), (e.g. Fig. 13b and d) the final state will depend on the subsequent decay of the χ . Neutralinos can undergo the \tilde{R}_p decays $\chi_\alpha^0 \rightarrow e^\pm q \bar{q}'$ or $\chi_\alpha^0 \rightarrow \nu q \bar{q}$, the former (latter) being dominant if χ_α^0 is dominated by its photino (zino) component. When χ_α^0 decays via \tilde{R}_p into a charged lepton, both the “right” and the “wrong” sign lepton (compared to incident beam) are equally probable leading to largely background free striking signatures for lepton number violation. On the contrary, the only \tilde{R}_p decays for charginos are $\chi_\alpha^\pm \rightarrow \nu u^j \bar{d}^k$ and $\chi_\alpha^\pm \rightarrow e^+ d^k \bar{d}^j$. Neutralinos χ_α^0 with $\alpha > 1$ as well as

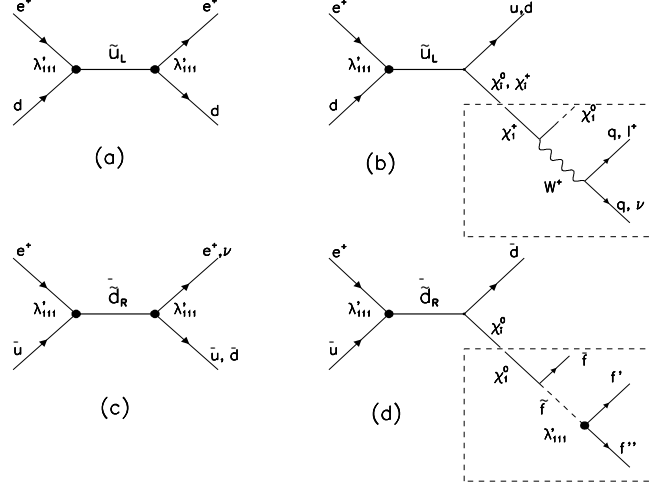
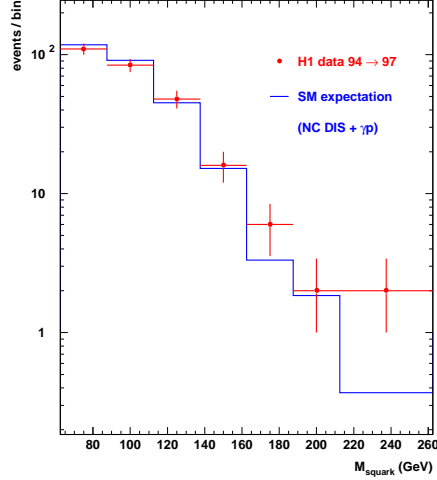


Figure 13: Lowest order s -channel diagrams for first generation squark production at HERA followed by (a),(c) \tilde{H}_p decays and (b),(d) gauge decays. In (b) and (d), the emerging neutralino or chargino might subsequently undergo \tilde{H}_p decays of which examples are shown in the dashed boxes for (b) the χ_1^0 and (d) the χ_1^0 .

charginos can also undergo gauge decays into a lighter χ and two SM fermions, through a real or virtual gauge boson or sfermion.

Event topologies: Overall, a e^\pm +multijets final state configuration is a likely one for a significant part of the MSSM parameter space when considering squark gauge decays, as discussed in previous HERA analysis^{35,36}. Such event topologies have been searched by H1 requiring an isolated e^\pm found at large y_e ($y_e > 0.4$) while, nevertheless, being accompanied by 2 forward (relative to the incident proton direction) high E_T jets. Such a configuration is very unlikely for standard NC DIS. H1 finds 289 candidates in the e^\pm +multijets channel, in good agreement with the mean SM background of 285.7 ± 28.0 expected from NC DIS and photoproduction (the latter contributes to less than 3%). The measured mass spectrum of the S3 selected events is compared to SM expectation in Fig. 14. Good agreement is observed with only a slight excess of events observed at the highest masses. H1 has further looked for “wrong” sign final state lepton in the process $e^+q' \rightarrow \tilde{q} \rightarrow e^-q''\bar{q}''q'$. One such wrong sign candidate was observed in the data, while the SM prediction as estimated from Monte-Carlo was found to be 0.49 ± 0.2 (coming from NC DIS). Hence, apart from an excess of NC-like events at large Q_e^2 or large M_e , no significant

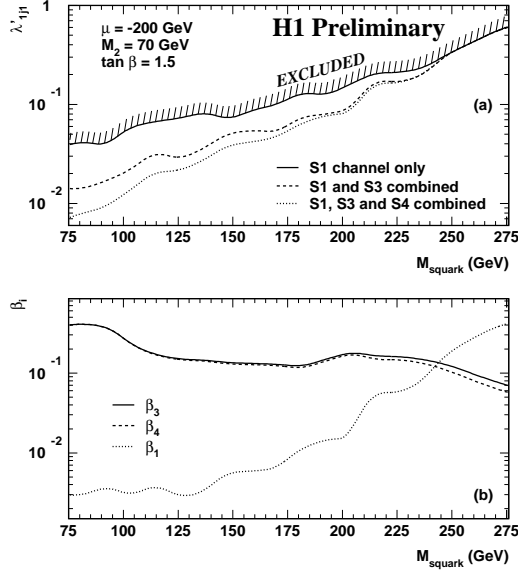
Figure 14: Mass spectrum for $e + \text{multijets}$ final states for data (symbols) and NC DIS expectation (histogram).



deviation from the SM expectations has been found in a key topology for gauge decay channels. Assuming that the slight deviations observed are due to statistical fluctuations, the searches in \tilde{R}_p and gauge decay channels can be combined to set constraints on \tilde{R}_p -SUSY models.

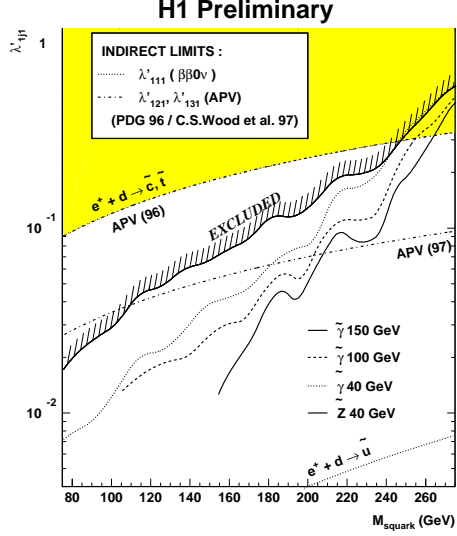
Rejection limits: The rejection limits are derived as a function of the \tilde{u}_L^j mass assuming that only one of the λ'_{1j1} is non vanishing and combining all contributing channels. The masses of other sfermions are assumed to only influence weakly the branching ratios of the neutralinos and charginos³⁴. Rejection limits on λ'_{1j1} as a function of squark mass are shown in Fig. 15a for the \tilde{u}_L^j when combining the relevant event topologies, taking into account either NC-like e^+ +jet only, or NC-like e^+ +jet combined with e^+ +multijets, or all three channels (including “wrong sign” e^- +multijets). The MSSM parameters have been set here to $\mu = -200$ GeV, $M_2 = 70$ GeV and $\tan\beta = 1.5$. With this choice of parameters, the lightest neutralino χ_1^0 is mainly dominated by its photino ($\tilde{\gamma}$) component and $M_{\chi_1^0} \simeq 40$ GeV, while the χ_1^+ and χ_2^0 are nearly degenerate around 90 GeV. Combining the three contributing channels improves the sensitivity on λ'_{1j1} by up to a factor $\simeq 5$ at lowest mass compared to the one obtained using only the NC-like channel. The relative contributions of the three channels in the case where χ_1^0 is $\tilde{\gamma}$ -like are plotted against the squark mass in Fig. 15b for λ' at the current sensitivity limit. It is seen that for masses up to $\simeq 230$ GeV, the channels e^+ +multijets and e^- +multijets

Figure 15: (a) Exclusion upper limits at 95% CL for λ'_{1j1} as a function of the $M_{\tilde{q}}$, for a set of MSSM parameters leading to a 40 GeV χ_1^0 dominated by its $\tilde{\gamma}$ component. The limits are given for different possible combinations of the contributing channels. Regions above the curves are excluded. (b) The relative contributions of channels e^+ +jet (S1), e^+ +multijets (S3) and e^- +multijets (S4) versus $M_{\tilde{q}}$.



have equal and dominant contributions. These channels play a decreasing role with increasing $M_{\tilde{q}}$ as squark decays into χ_1^+ and χ_2^0 become kinematically allowed. The χ_1^+ and χ_2^0 become dominated respectively by their wino and zino components^{35,36} and decay preferentially into $\nu q \bar{q}$ (a channel not covered in ref.³³ except partly through CC-like analysis). In the very high mass domain, a large Yukawa coupling is necessary to allow squark production, hence the relative contribution of e^+ +jet is largely enhanced. Another set of values for $(\mu, M_2, \tan \beta)$ leading to a 40 GeV χ_1^0 dominated by its zino (\tilde{Z}) component was considered in³³ to study the dependence of the rejection limits on the choice of MSSM parameters. In such a case the χ_1^0 of the χ_1^+ decay preferably in $\nu q \bar{q}$ (rather than in eqq'), leading to multijets+ $P_{T,miss}^{vis.}$ topologies not easily separable from the SM background^{35,36} and, hence, not expected to contribute very much to the sensitivity to new physics. Since the gauge decay width of the squark does not depend on the Yukawa coupling λ'_{1j1} , the region of the plane $(\beta_1, M_{\tilde{q}})$ above the dotted line in Fig. 15b is excluded at 95% CL by H1 combined analysis. In particular the branching ratio of a 200 GeV \tilde{u}_L^j squark into $e^+ + q$ is constrained to be smaller than $\simeq 1.5\%$ (Fig. 15b) for the MSSM parameter choice presented here. It should be noted however that other spe-

Figure 16: Exclusion upper limits at 95% CL for the coupling λ'_{1j1} as a function of squark mass, for various masses and mixtures of the χ_1^0 ; also represented are the most stringent indirect limits on λ'_{111} and λ'_{1j1} , $j = 2, 3$.



cific choices of $(M_2, \mu, \tan \beta)$ can allow for squarks at ~ 200 GeV to lead to NC-like topologies with $\beta_{eq} \gtrsim 10\%$.

Rejection limits obtained at HERA depending on the χ_1^0 mass and nature are compared in Fig. 16. The sensitivity to λ'_{1j1} for $M_{\tilde{q}} \lesssim 200$ GeV is better by a factor $\simeq 2$ for a $\tilde{\gamma}$ -like χ_1^0 than for a χ_1^0 dominated by its \tilde{Z} component, due to the highest part of total branching actually “seen” in the H1 analysis³³. One can infer from previous \tilde{R}_p -SUSY searches at HERA³⁵ that the two cases presented here are somewhat “extreme” and in that sense quite representative of the sensitivity at HERA for any other choice of MSSM parameters leading to a $\simeq 40$ GeV χ_1^0 . The sensitivity to λ'_{1j1} for $\tilde{\gamma}$ -like χ_1^0 increases with $M_{\tilde{\gamma}}$ given the corresponding increase of efficiency for the e +multijets channels. For $\lambda_{1j1} = \sqrt{4\pi\alpha_{em}}$, squark masses up to 262 GeV are excluded at 95% CL by this analysis, and up to 175 GeV for coupling strengths $\simeq 0.01\alpha_{em}$. For low masses, these limits represent an improvement of a factor $\simeq 3$ compared to H1 previously published results³⁵.

Other indirect and direct constraints: The rejection limits obtained at HERA are compared to the best indirect limits in Fig. 16. The most stringent indirect constraint comes from the non-observation of neutrinoless double beta decay³⁷ but only concerns λ'_{111} coupling. The most severe indirect limits³⁸ on couplings λ'_{121} and λ'_{131} , which could allow for the production of

squarks \tilde{c} and \tilde{t} respectively, come from APV²¹. It is seen that the sensitivity at HERA is better or comparable to the most stringent constraints on λ'_{121} and λ'_{131} . For large $M_{\chi_1^0}$ values, HERA limits improves the sensitivity on some λ' coupling by a factor up to $\simeq 4$.

LQ-like searches imply stringent constraints on \tilde{u}_L^j squark masses only if somehow β_{eq} can be made large. But as explained above, this is unlikely in \tilde{R}_p -SUSY for (say) $M_{\tilde{q}} \simeq 200$ GeV. Hence, LQ-like constraints from the Tevatron are easily evaded. The problem is that a small β_{eq} is so natural in \tilde{R}_p -SUSY⁴ that, at first glance, only a minute portion of the MSSM parameter space is left if one would like to “explain” a NC-like signal at $M \simeq 200$ GeV in e^+p collisions via the production of a \tilde{u}_L -like squark (e.g. \tilde{c}_L or \tilde{t}_L). Actually, elegant solutions can be found as discussed below in the case of the \tilde{t}_L . At the TeVatron, SUSY searches have been mainly carried in the framework of minimal Supergravity (SUGRA) which imposes mass relations between the sparticles and R -parity conservation. Recently, $D\emptyset$ ³⁹ also considered squark pair production leading in \tilde{R}_p -SUGRA to like-sign dielectron events accompanied by jets, and has ruled out $M_{\tilde{q}} < 252$ GeV (95 % CL) when assuming five degenerate squark flavours. From a similar analysis by CDF⁴⁰ restricted to $\lambda'_{121} \neq 0$, one can infer that a cross-section five times smaller would lead to a $M_{\tilde{q}}$ limit of $\simeq 150$ GeV depending on the gluino and χ^0 masses. CDF also considered separately⁴⁰ the pair production of a light stop \tilde{t}_1 assuming a decay into $c\chi_1^0$ and excluded $M_{\tilde{t}} < 130$ GeV. To translate this constraint in one relevant for $\lambda'_{13k} \neq 0$, it should be noted that in this latter case, \tilde{R}_p -decays of the \tilde{t} would dominate over loop decays into $c\chi_1^0$. Moreover, \tilde{R}_p -decays would themselves be negligible compared to $\tilde{t} \rightarrow b\chi_1^+$ decays as soon as this becomes allowed, i.e. if $M(\tilde{t}_1) > M(\chi_1^+)$ and if the \tilde{t}_1 eigenstate possesses a sizeable admixture of \tilde{t}_L . The subsequent decays of the χ_1^+ would then lead to final states similar to those studied by CDF for $\tilde{t}_1 \rightarrow c\chi_1^0$. Thus, 130 – 150 GeV appears to be reasonable rough estimate of the TeVatron sensitivity to a light \tilde{t} for $\lambda'_{13k} \neq 0$. In summary, TeVatron and HERA sensitivities are competitive in \tilde{R}_p -SUSY models with five degenerate squarks, but models predicting a light \tilde{t} are better constrained at HERA provided that λ'_{13j} is not too small.

Now let's come back to the case of the \tilde{t}_L . Sizeable branching ratios for both \tilde{R}_p and gauge decay modes for a \tilde{t} produced via λ'_{131} are very difficult to realize as argued in⁴¹ when restricting to \tilde{t} decays into $e + d$ and $b + \chi_1^+$. In particular, the conflicting requirements due to APV²¹ constraints (implying a lower bound for β_{eq}) and to direct searches at the TeVatron (implying an upper bound on β_{eq}) are not easily accommodated. A special case occurs if there exists a very heavy χ_1^+ ($M_{\chi^+} > M_{\tilde{t}}$) and a light \tilde{b} ($M_{\tilde{b}} < M_{\tilde{t}}$) such that the \tilde{t} is left with the decay modes $\tilde{t} \rightarrow e^+d$ and $\tilde{t} \rightarrow \tilde{b}W^+$. This interesting possibility

was first discussed in ⁴² as a way to “explain” simultaneously an excess in the NC-like channel and the striking observation ²⁹ of LFV-like events with high $P_{T,miss}^{vis.}$ containing a high P_T muon and jet(s). For a lightest \tilde{b} mass $\simeq 100$ GeV, simultaneous sizeable branching ratios β_{e+d} and β_{bW^+} become possible ⁴³ for the \tilde{t} thus extending the discovery potential at HERA for $M_{\tilde{t}} \simeq 200 - 250$ GeV.

7 Conclusions

The recent observation of possible deviations from Standard Model expectation in electroweak-like processes at HERA has considerably revived the interest in new theories requiring bosons with Yukawa couplings to lepton-quark pairs. Collider experiments and low energy precision experiments have reached remarkable (and often comparable) sensitivity to such particles, providing new avenues for the manifestation of exciting new physics.

Acknowledgments

I wish to thank the organizers of the WEIN 98 Conference and the Chairman Prof. Cyrus Hoffman for providing me with this opportunity to discuss the exciting prospects at HERA and other colliders for new physics closely linked to the symmetry between the leptonic and quarkonic sectors of standard matter. I wish to thank members of the H1 and ZEUS Collaborations for their support.

References

1. H1 Collab., C. Adloff *et al.*, Z. Phys. C74 (1997) 191.
2. ZEUS Collab., J. Breitweg *et al.*, Z. Phys. C74 (1997) 207.
3. K.S. Babu *et al.*, Phys. Lett. B402 (1997) 367; J.L. Hewett and T.G. Rizzo, Phys. Lett. B403 (1997) 353; T. Plehn *et al.*, Z. Phys. C74 (1997) 611; C. Friberg *et al.*, Phys. Lett. B403 (1997) 329; J.K. Ellwood and A.E. Faraggi, Nucl. Phys. B512 (1998) 42; E. Keith and E. Ma, Phys. Rev. Lett. 79-22 (1997) 4318; N.G. Deshpande and B. Dutta, Phys. Lett. B424 (1998) 313; J.L. Hewett and T.G. Rizzo, Phys. Rev. D58 (1998) 55005; R. Ruckl and H. Spiesberger, Proc. Workshop on Physics Beyond the Desert, Tegernsee, Germany (8-14 June 1997) 18pp.; and references therein.
4. D. Choudhury and S. Raychaudhuri, Phys. Lett. B401 (1997) 54; G. Altarelli *et al.*, Nucl. Phys. B506 (1997) 3; H. Dreiner and P. Morawitz, Nucl. Phys. B503 (1997) 55; T. Kon and T. Kobayashi, Phys. Lett. B409 (1997) 265; G. Altarelli *et al.*, Nucl. Phys. B506 (1997) 29; J. Ellis *et al.*, Phys. Lett. B408 (1997) 252; J.E. Kim and

- P. Ko, Phys. Rev. D57 (1998) 489; R. Rückl, H. Spiesberger, Proc. Workshop New Trends in HERA Physics, Tegernsee, Germany (May 25-30, 1997) 14pp.; A. S. Joshipura *et al.*, Phys. Rev. D57 (1998) 5327; and references therein.
5. V. Barger *et al.*, Phys. Lett. B404 (1997) 147; M.C. Gonzalez-Garcia and S.F. Novaes, Phys. Lett. B407 (1997) 225; N.D. DiBartolomeo and F. Frabrichesi, Phys. Lett. B406 (1997) 237; A.N. Nelson, Phys. Rev. Lett. 78 (1997) 4159; W. Buchmüller and D. Wyler, Phys. Lett. B407 (1997) 147; N.G. Desphande *et al.*, Phys. Lett. B407 (1997) 288; and references therein.
 6. DØ Collab., B. Abbott *et al.*, Phys. Rev. Lett. 79 (1997) 4321; *idem* Phys. Rev. Lett. 80 (1998) 2051.
 7. CDF Collab., F. Abe *et al.*, Phys. Rev. Lett. 79 (1997) 4327.
 8. S. Bentvelsen *et al.*, Proc. Workshop on Physics at HERA, DESY-Hamburg (October 1991) Vol. 1 p. 25; K.C. Hoeger, *ibid.* p. 43.
 9. H1 Collab., XXIXth Int. Conf. on High Energy Physics (ICHEP98), Vancouver, Canada (22-30 July 1998), paper #533, 29pp.
 10. ZEUS Collab., ICHEP98, paper #751, 15pp.; *idem*, paper #752, 11pp.
 11. M. Drees, Phys. Lett. B403 (1997) 353; U. Bassler and G. Bernardi, Z. Phys. C76 (1997) 223.
 12. H1 Collab., ICHEP98, paper #579, 24pp.
 13. Ph. Bruel, LPNHE Ecole Polytechnique, Ph.D. Thesis, Université de Paris-Sud, Orsay (May 1998) 191pp.
 14. T. K. Kuo and T. Lee, Modern Phys. Lett. A12 (1997) 2367; Z. Kunszt and W. J. Stirling, Z. Phys. C75 (1997) 453; M. Heyssler and W.J. Stirling, Phys. Lett. B407 (1997) 259; V.V. Kiselev, Phys. Rev. D58 (1998) 54008; D. Bowser-Chao *et al.*, Phys. Lett. B432 (1998) 167.
 15. H.L. Lai *et al.*, Phys. Rev. D55 (1997) 1280.
 16. NMC Collab., M. Arneodo *et al.*, Phys. Lett. B364 (1995) 107.
 17. BCDMS Collab., A. Benvenuti *et al.*, Phys. Lett. B223 (1989) 485.
 18. H1 Collab., S. Aid *et al.*, Nucl. Phys. B470 (1996) 3; H1 Collab., Europhysics Conf. on High-Energy Physics (HEP97), Jerusalem, Israel (19-26 August 1997), paper # 260, 22pp.
 19. Ph. Bruel, H1 Collab., Proc. XXXIVth Renc. de Moriond: Electroweak Interactions and Unified Theories, Les Arcs, France (14-21 March 1998) 2pp.; M. Kuze, ZEUS Collab., *ibid.*, 6pp.
 20. B. Heinemann, H1 Collab., Proc. VIth Int. Workshop on Deep-Inelastic Scattering and QCD, Brussels, Belgium (4-8 April 1998) 7pp.
 21. P. Langacker, Phys. Lett. B256 (1991) 277; C.S. Wood *et al.*, Science 275 (1997) 1759.

22. H1 Collab., ICHEP98, paper #584, 8pp.; ZEUS Collab., *ibid*, paper #753, 14pp.
23. W. Buchmüller, R. Rückl and D. Wyler, Phys. Lett. B191 (1987) 442.
24. B. Schrempp, Proc. Workshop on Physics at HERA, DESY-Hamburg (October 1991) Vol. 2 p. 1034, and references therein.
25. S. Davidson *et al.*, Z. Phys. C61 (1994) 613; M. Leurer, Phys. Rev. D49 (1994) 333.
26. H1 Collab., I. Abt *et al.*, Nucl. Phys. B396 (1993) 3. H1 Collab., T. Ahmed *et al.*, Z. Phys. C64 (1994) 545; H1 Collab., S. Aid *et al.*, Phys. Lett. B369 (1996) 173. ZEUS Collab., M. Derrick *et al.*, Phys. Lett B306 (1993) 173. ZEUS Collab., M. Derrick *et al.*, Proc. Int. High Energy Physics, Glasgow, Vol. 2 (1994) 797.
27. CDF and D0 Collab., Carla Grosso-Pilcher *et al.*, eprint hep-ex/9810015, (October 1998) 9pp.
28. DELPHI Collab., HEP97, paper #352; OPAL Collab., *ibid* paper #205.
29. H1 Collab., C. Adloff *et al.*, Eur. Phys. J. C5 (1998) 575.
30. CDF Collab., F. Abe *et al.*, Phys. Rev. Lett. 78 (1997) 2906.
31. DØ Collab., B. Abbott *et al.*, Phys. Rev. Lett. 81 (1998) 38.
32. ZEUS Collab., M. Derrick *et al.*, Z. Phys. C73 (1997) 613.
33. H1 Collab., ICHEP98, paper #580, 23pp.
34. J. Butterworth and H. Dreiner, Nucl. Phys. B397 (1993) 3; H. Dreiner, P. Morawitz, Nucl. Phys. B428(1994) 31.
35. H1 Collab., T. Ahmed *et al.*, Z. Phys. C64 (1994) 545; H1 Collab., S. Aid *et al.*, Z. Phys. C71 (1996) 211.
36. E. Perez and Y. Sirois, Proc. Workshop on Dark Matter in Astro- and Particle Physics, Heidelberg, Germany (16-20 September 1996) 615.
37. R.N. Mohapatra, Phys. Rev. D34 (1986) 3457. J.D. Vergados, Phys. Lett. B184 (1987) 55; M. Hirsch *et al.*, Phys. Lett. B352 (1995) 1.; *idem*, Phys. Rev. Lett. 75 (1995) 17.
38. For a recent review of indirect constraints on R_p -violating couplings see for instance R. Barbier *et al.*, R-Parity Violating Group, GDR-SUSY/CNRS, eprint hep-ph/9810232 (October 1998) 60pp.
39. DØ Collab., Contrib. paper #588, XXIX Int. Conf. on High Energy Physics, Vancouver, Canada (23-29 July 1998)
40. M. Chertok, for DØ and CDF Collab., Proc. XXXIIIrd Renc. de Moriond, QCD and High Energy Hadronic Interactions, Les Arcs, France, (March 21-28, 1998) 6pp.
41. G. Altarelli *et al.*, Nucl. Phys. B506 (1997) 3.
42. T. Kon *et al.*, Mod. Phys. Lett. A12 (1997) 3143.
43. E. Perez, Talk at SUSY98 Conf., Oxford, England (11-17 July 1998)